Chapter 1
Rare Earth, Rare Earth Luminescence, Luminescent Rare Earth Compounds, and Photofunctional Rare Earth Hybrid Materials

Abstract This chapter mainly focuses on the fundamental principles of rare earth luminescence, which are important for the investigation of the photofunctional rare earth hybrid materials. It introduces the rare earth elements and their physiochemical properties, the atomic spectral term and energy level transition of rare earth ions associated with their electronic configuration, and the luminescence and spectroscopy of rare earth ions, rare earth inorganic compounds for phosphors, rare earth coordination compounds for molecular luminescence, and photofunctional rare earth hybrid materials combining the characteristics of both phosphor and molecular luminescence. This chapter provides a basis to understand the contents of the subsequent chapters.

Keywords Rare earth ion • Luminescence • Energy transfer • Phosphor • Complex • Photofunctional hybrid material

1.1 Introduction

Rare earths (REs) are a special group of elements in the periodic table, consisting of sixth-period lanthanides, fourth-period scandium (Sc), and fifth-period yttrium (Y). The lanthanides are a series of elements with atomic numbers from 57 to 71, including lanthanum (La), cerium (Ce), praseodymium (Pr), neodymium (Nd), samarium (Sm), europium (Eu), gadolinium (Gd), terbium (Tb), dysprosium (Dy), holmium (Ho), erbium (Er), thulium (Tm), ytterbium (Yb), and lutetium (Lu). Sc and Y possess the nearly identical chemical properties as lanthanides, although lacking in 4f electrons, so they occur in the same ore bodies and have the same separation difficulties. Therefore, they are usually included in the rare earth category.

The rare earths can be generally divided into two classes, the "light rare earth elements (LREE)" (Ce fraction) and "heavy rare earth elements (HREE)" (Y fraction), i.e., $<4f^7$ and $>4f^7$, respectively. Historically, the two classes were from different ores and studied independently. Y is a heavy rare earth element for its physicochemical property similar to Ho and Er. There are slight differences in physicochemical properties from each other which follow this rule of light and heavy

B. Yan, *Photofunctional Rare Earth Hybrid Materials*,
Springer Series in Materials Science 251, DOI 10.1007/978-981-10-2957-8_1

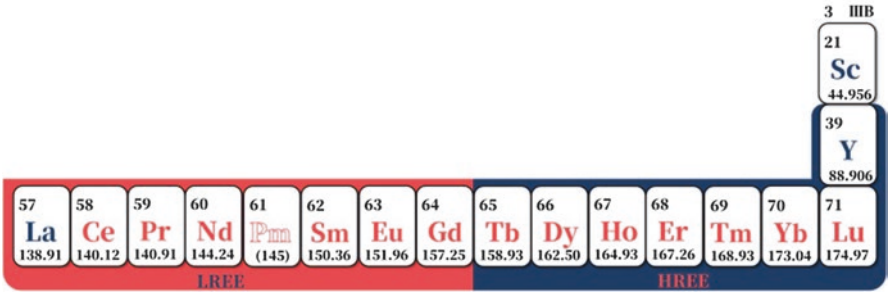

Fig. 1.1 The rare earth elements are often subdivided into light rare earth elements (LREE) and heavy rare earth elements (HREE)

rare earth elements as well. The term "rare earths" has been historically applied to the lanthanides because it was originally believed that these elements were sporadically distributed in nature. But in fact, some elements among them, such as La, Ce, and Y, are relatively abundant (Fig. 1.1) [1].

One important rule correlating structure and physicochemical property of rare earth elements is so-called lanthanide contraction, a term used in chemistry to describe different but closely related concepts associated with smaller than expected atomic radii of the elements in the lanthanide series [2]. In multi-electron atoms, the decrease in radius brought about by increase in nuclear charge is partially offset by electrostatic repulsion among electrons. Particularly, a "shielding effect" operates, i.e., as electrons are added in outer shells, electrons already present shield the outer electrons from nuclear charge, making them a lower effective charge on the nucleus. The shielding effect exerted by the inner electrons decreases in order s > p > d > f. Usually when a particular subshell is filled up in a period, the atomic radii decrease. This effect is particularly pronounced in the case of lanthanides as their 4f subshells are being filled across the period, and they are least able to shield two outer (fifth and sixth) shell electrons. Thus, the shielding effect is least able to counter the decrease in radii caused by the increasing nuclear charge, which leads to "lanthanide contraction." Radius drops from 1.020 Å in the case of Ce (III) to 0.861 Å in the case of Lu (III) [2]. Since the outer shells of the lanthanides do not change within the group, their chemical behavior is very similar, but the different atomic and ionic radii do affect their chemistry. Without the lanthanide contraction, the chemical separation of lanthanides will be extremely difficult. However, this contraction makes the chemical separation of period 5 and period 6 transition metals of the same group rather difficult. All elements following the lanthanides in the periodic table are influenced by the lanthanide contraction. The period 6 elements have very similar radii compared with the period 5 elements in the same group [2].

Rare earth elements are commonly associated to accessory minerals presenting structures that are large enough. They present high ionic charge and associated large ionic radius. They correspond to transition metals ranging from $4f^0$ to $4f^{14}$, since they progressively fill the $4f$ electronic shell. Chemical properties slowly vary from La to Lu, according to their decreasing ionic radius. The trend usually decreases

from LREE to HREE. However, within the 15 elements of the group, the respective ionization potentials present large variations. Values increase first, correlating with the increase in nuclear charge, which in turns increases the repulsion between electrons. However, a break is observed between f^6 and f^7, i.e., Eu and Gd, caused by the exchange of energy resulting from coupling between paired electrons. It represents the half shell effect. Similar effects, but with reduced amplitude, occur at quarter and three-quarter filling of the electronic shell. REE are subdivided to four groups (or tetrads) containing four elements each. The four groups include La to Nd, Pm to Gd, Gd to Ho, and Er to Lu. The four tetrads present specific variations superimposed to the linear trend from LREE to HREE. In each group, the tetrad effect is superimposed on the linear trend and manifested by a curved shape that develops on the four elements. But, depending on the chemical reactions that involve RE elements, those can be more favorably incorporated or not to the mineral assemblage. Two mutually opposite effects are observed, noted W and M types [3].

Here we only give a special example to demonstrate the lanthanide contraction and tetrad effect, which is shown in the cyano-bridged aqua (N,N-dimethylacetamide) (cyanometal) rare earth (Sm, Gd, Ho, Er) nitrate and potassium hexacyanometallate. There are four typical different coordination geometries and crystal structures in these series of complexes with the same terminal ligand N,N-dimethylacetamide (DMA): one-dimensional chain for Sm $\{[Sm(DMA)_2(H_2O)_4Fe(CN)_6{\cdot}5H_2O]_n$, $[SmFe]_n\}$ with approximately parallel transpositioned bridging CN ligands between the Sm and Fe atoms, trinuclear for Gd $([(Gd(DMA)_3(H_2O)_4)_2Fe(CN)_6][Fe(CN)_6]{\cdot}3H_2O$, Gd_2Fe) with two approximately perpendicular cis-positioned bridging CN ligands between the two Gd and Fe atoms, homonuclear for Ho $([Ho(DMA)_3(H_2O)_3Fe(CN)_6]{\cdot}3H_2O$, HoFe) with only one bridging CN between the Ho and Fe atom, and ion pair for Er $([Er(DMA)_3(H_2O)_4][Cr(CN)_6]$, Er-Cr) without any CN bridging between Er and Cr atoms [4, 5].

Besides, there also exists some special phenomenon, which depends on the physiochemical property of rare earth compounds. For example, in the synthesis of $NaRE(MoO_4)_2$ (RE = Y, La, Nd, Eu, Gd, Tb, Er, Yb) and $Na_5Lu(MoO_4)_4$ compounds by a room-temperature solid-state reaction and hydrothermal crystallization process, it indicates that the higher temperature and moisture can speed up the reaction process, and especially the existence of crystalline water molecules in the precursor is necessary for the solid-state reaction at room temperature. It is found that different rare earth nitrate precursors present the different reactivity to sodium molybdate at room temperature. The crystallization degree of the products after room-temperature solid-state reaction depends on the melting point of rare earth nitrate precursors [6].

For rare earth atoms, their electronic configurations are Sc $1s^22s^22p^63s^23p^63d^14s^2$, Y $1s^22s^22p^63s^23p^63d^{10}4s^24p^64d^15s^2$, and Ln $1s^22s^22p^63s^23p^63d^{10}4s^24p^64d^{10}4f^n5s^25p^65d^m6s^2$ ($m = 0, 1$; $n = 0$–14). For trivalent rare earth ions, their electronic configurations are Sc(III) $1s^22s^22p^63s^23p^6$, Y(III) $1s^22s^22p^63s^23p^63d^{10}4s^24p^6$, and Ln(III) $1s^22s^22p^63s^23p^63d^{10}4s^24p^64d^{10}4f^n5s^25p^6$ (n = 0–14; among Ln = La, Ce, Gd, and Lu: $5d^1$). Besides the common trivalent state, some rare earth elements can form the divalent (Eu(II), Sm(II), Tm(II), Yb(II)) and tetravalent (Ce(IV) (CeO_2), Pr(IV)

(Pr_6O_{11}), Tb(IV) (Tb_4O_7)) under normal conditions. In aqueous solution, only Ce(IV), Eu(II), and Yb(II) can exist stably.

1.2 Atomic Spectral Term and Energy Level Transition of Rare Earth Ions

The incompletely filled 4f shell of rare earth ions possesses single electrons and produces the non-zero spin quantum number (S). So the spin angular momentum splits and disturbs the orbital angular momentum (L) in the same space region, resulting in the fine splitting of orbital energy levels, so-called the spin–orbit coupling effect. Rare earth ions possess many single electrons and show large quantum number, whose spin–orbit coupling effect is strong. Therefore, the common spectral term $^{2S+1}$L-based S and L cannot show the fine energy levels of rare earth ions; we have to consider the strong spin–orbit coupling effect and introduce the angular quantum number (J) originated from L and S. Subsequently, the electron configurations and energy levels of rare earth ions are presented as a spectral sub-term $^{2S+1}L_J$.

For all the rare earth ions, the number of single electrons in the 4f orbital shows the symmetrical distribution centered with Gd^{3+} ion, so there is a rule for their quantum number (L and S). For L and J, a so-called gadolinium breaking effect shows the two different formulas: in front of Gd^{3+}, J = L-S, $L = -1/2(n(n-7))$ and behind Gd^{3+}, J = L + S, $L = -1/2((n-7)(n-14))$, where L can be represented as S, P, D, F, G, H, and I, respectively. So being centered with Gd^{3+}, the light rare earth ion and the heavy one show the same L and S symmetrically except for the different J.

Figure 1.2 presents a substantial part of the energy levels originating from the $4f^n$ configuration as a function of n for the trivalent rare earth ions; the width of the bars in the figure gives the order of magnitude of the crystal field splitting. So the number of possible energy level transitions for these rare earth ions is great, revealing that rare earth ions and their compounds are a huge treasure of luminescent materials [7].

1.3 Luminescence and Spectroscopy of Rare Earth Ions

Trivalent rare earth ions such as Sc^{3+}, Y^{3+}, La^{3+}, and Lu^{3+} possess the stable, empty, or filled state, so they are optically inert ions and cannot show the photoactive behavior. Gd^{3+} has half-empty 4f shell and produces a very stable $^8S_{7/2}$ ground state with excitation energy higher than 32,000 cm^{-1}, so the emission of Gd^{3+} is situated in the ultraviolet region (<318 nm). $^8S_{7/2}$ level belongs to non-degenerate orbital and cannot be split by the crystal field, and so its low-temperature emission spectrum only shows a line peak originated from the transition ($^6P_{7/2} \rightarrow {}^8S_{7/2}$). Although Gd^{3+} has the same electron configuration as Eu^{2+}, its $4f^65d$ state is situated at a relatively

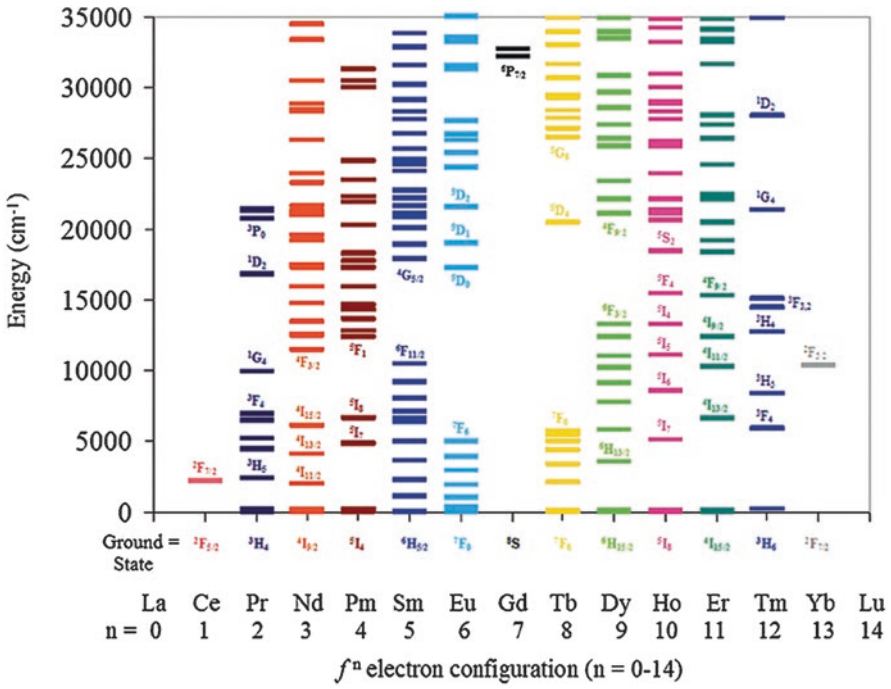

Fig. 1.2 A summary of electronic excited state energy levels for RE^{3+} ions. Reprinted with permission from Ref. [7]. Copyright 2009 the American Chemical Society

high energy state, and it is impossible to observe the band emission from $4f^6 5d \rightarrow 4f^7$ transition. The luminescence of Gd^{3+} mainly comes from $^6P \rightarrow {}^8S$ transition, a line emission at 313 nm. At its high-energy position, the transition emission can be observed in the host lattice with high-energy optical absorption. Besides, the energy transfer is easy from the ^6P energy level of Gd^{3+} to other rare earth ions or host lattice groups. Therefore, Gd^{3+} generally is considered as an inert ion just like Sc^{3+}, Y^{3+}, La^{3+}, and Lu^{3+} [8, 9].

The emission spectral lines of Eu^{3+} are situated in a red color region, which correspond to the transitions ($4f^6$) from excited state $^5D_0$ to ^7F_J (J = 0, 1, 2, 3, 4, 5, 6). Because the $^5D_0$ level cannot be split by the crystal field (J = 0), the crystal field splitting of ^7F_J levels is produced by the splitting of the emission transitions. Besides, the emission from the higher ^5D energy level ($^5D_1$, $^5D_2$, $^5D_3$) can also be observed. $^5D_0 \rightarrow {}^7F_J$ emission is suitable to determine the spectral features of Eu^{3+}. If Eu^{3+} is located in the lattice with inversion symmetry, electric-dipole transitions between levels of $4f^n$ configuration are strictly forbidden by parity selection rule, and only the weak magnetic-dipole transitions or vibronic electric-dipole transitions occur. If Eu^{3+} is situated in the lattice without inversion symmetry, electric-dipole transition is not strictly forbidden and shows weak spectral lines, so-called forced electric-dipole transition. These transition emissions need two conditions: one is the

crystallographic lattice of Eu^{3+} does not have an inversion symmetry center, and the other is the charge transition state which is situated at the low energy level [8, 10].

According to the split number of ^7F_J energy level and the transition number of $^5D_0 \rightarrow {}^7F_J$ transition, it is easy to predict the point group symmetry of the environment where Eu^{3+} is situated: (a) When Eu^{3+} is situated in the lattice with a strict inversion symmetry center, the allowed magnetic-dipole transition $^5D_0 \rightarrow {}^7F_1$ with orange light (about 590 nm) is dominant. (b) When Eu^{3+} is situated in the point group symmetry C_i, C_{2h} and D_{2h}, its $^5D_0 \rightarrow {}^7F_1$ transition shows three spectral lines for the splitting of three states from the completely removed degeneration of $^7F_1$ level in symmetric crystal field. (c) When Eu^{3+} is situated in the point group symmetry C_{4h}, D_{4h}, D_{3d}, S_6, C_{6h}, and D_{6h}, its $^7F_1$ level splits into two states to show two$^5D_0 \rightarrow {}^7F_1$ transition spectral lines. (d) When Eu^{3+} is situated in the point group symmetry T_h and O_h with a high cubic symmetry, $^7F_1$ level only has one split and shows one $^5D_0 \rightarrow {}^7F_1$ transition spectral line.

On the other hand, when Eu^{3+} is situated in the lattice with deviated inversion symmetry center, the forbidden electric-dipole transition $^5D_0 \rightarrow {}^7F_0$ with red light (about 615 nm) is dominant: (a) When Eu^{3+} is situated in the point group symmetry C_s, C_n, and C_{nv}, its $^5D_0 \rightarrow {}^7F_0$ transition emission appears at 580 nm because the expanding crystal field potential energy surface transition needs to involve odd-order crystal field term. (b) $^5D_0 \rightarrow {}^7F_0$ transition of Eu^{3+} cannot be split by the crystal field and shows only one emission peak, and then each peak corresponds to one crystal lattice. Therefore, the number of $^5D_0 \rightarrow {}^7F_1$ emission peaks can be utilized to predict the lattice number of point group symmetry where Eu^{3+} is located (C_s, C_n, and C_{nv}). (c) When Eu^{3+} is situated in point groups with low symmetry, such as triclinic crystal system C_1 and monoclinic crystal system C_s, C_2, $^7F_1$, and $^7F_2$ levels completely remove the degeneration state and are split into three and five sublevels, respectively. Subsequently, there are one $^5D_0 \rightarrow {}^7F_0$ peak, three $^5D_0 \rightarrow {}^7F_1$ peaks, and five $^5D_0 \rightarrow {}^7F_2$ peaks, respectively; among them $^5D_0 \rightarrow {}^7F_2$ transition shows the dominant red emission.

Tb^{3+} emission has originated from its $^5D_4 \rightarrow {}^7F_J$ transition, mainly in the green color region. Besides, the $^5D_3 \rightarrow {}^7F_J$ transition from the high energy level also shows an emission mainly in blue region, which is easily quenched by the crossing relaxation energy transfer process $Tb(^5D_3) + Tb(^7F_6) \rightarrow Tb(^5D_4) + Tb(^7F_6)$. Sm^{3+} emission is situated in the orange–red color region, corresponding to $^4G_{5/2} \rightarrow {}^6H_J$ (J = 5/2, 7/2, 9/2, 11/2, 13/2) [11]. Dy^{3+} shows two main emissions in visible light region, corresponding to $^4F_{9/2} \rightarrow {}^6H_{15/2}$ (470–500 nm, blue region) and $^4F_{9/2} \rightarrow {}^6H_{13/2}$ (570–600 nm, yellow region) [12]. Among them the yellow emission $^4F_{9/2} \rightarrow {}^6H_{13/2}$ (570–600 nm) belongs to hypersensitive transition. The luminescence color of Dy^{3+} often is close to white. When the hypersensitive transition of host lattice is dominant, it shows yellow color emission. The yellow/blue (Y/B) ratio is the important luminescence parameters. The direct excitation of Dy^{3+} in ultraviolet region is not successful because its charge transfer state and 5d energy level are both over 50,000 cm^{-1}. During the energy transfer from host lattice to Dy^{3+}, only YVO_4: Dy^{3+} shows highly effective luminescence.

Pr^{3+} emission color strongly depends on the host lattice of doped Pr^{3+}. Red emission derives from its $^1D_2$ level, and green color emission comes from its $^3P_0$ level. Besides, it can also show blue emission from $^1S_0$ level and visible emission from $^4f^5d$ state [12]. Nd^{3+} ($4f^3$), Er^{3+} ($4f^{11}$), and Yb^{3+} ($4f^{13}$) often show the emission in near-infrared (NIR) region. For Nd^{3+}, its emission is ascribed to three transitions of $^4F_{3/2} \rightarrow {}^4I_J$ (J = 9/2, 11/2, and 13/2) [12]. For Yb^{3+}, it shows the typical emission coming from its $^2F_{5/2} \rightarrow {}^2F_{7/2}$ transition. For Er^{3+}, it exhibits emission in both NIR regions ($^4I_{13/2} \rightarrow {}^4I_{15/2}$) and visible region ($^2H_{11/2} \rightarrow {}^4I_{15/2}$ and $^4S_{3/2} \rightarrow {}^4I_{15/2}$ transition) [12]. Tm^{3+} shows a weak blue emission originating from $^1G_4 \rightarrow {}^3H_6$ transition [12].

Besides the line emission, some rare earth ions also show the wideband emission, such as trivalent ions (Ce^{3+}, Pr^{3+}, and Nd^{3+}) and divalent ions (Eu^{2+}, Sm^{2+}, and Yb^{2+}). Ce^{3+} has only one 4f electron with excited state electron configuration $5d^1$, whose ground state $4f^1$ contains two energy levels ($^2F_{5/2}$ and $^2F_{7/2}$). So Ce^{3+} exhibits two 5d → 4f transition emissions. Ce^{3+} emission generally is situated at ultraviolet or blue region. In few systems, the long wavelength emission in green or red region also can be found, in which the $5d^1$ energy level is relatively low and the crystal field strength is high [13]. The most popular divalent ion is Eu^{2+} ($4f^7$), whose 5d → 4f emission changes in the rage from long wavelength ultraviolet to yellow regions. Eu^{2+} mainly shows the wideband emission due to $4f^6 5d \rightarrow 4f^7$ transition, which also shows line emission under low-temperature condition [14].

1.4 Rare Earth Phosphors

Rare earth ions and their compounds are a huge treasure of luminescent materials, which can behave as both photoactive ions and host elements. Almost all kinds of rare earth ions can be utilized in phosphors. Rare earth phosphors become the most useful species for commercial applications, due to their typical luminescence processes and mechanisms.

Trivalent rare earth ions have excellent photoactive properties such as sharp emission spectra for high color purity, broad emission bands covering the ultraviolet (UV)-visible–near-infrared (NIR) region, a wide range of lifetimes from the microsecond to the second level, high luminescence quantum efficiencies, etc. These properties have attracted much attention for a wide variety of applications in the fields of lighting devices (television and computer displays, optical fibers, optical amplifiers, lasers) and biomedical analysis (medical diagnosis and cell imaging).

However, it is difficult for rare earth ions to directly behave as luminescent materials because of their poor light absorption abilities. As it is known, the f–f transitions of rare earth ions are spin forbidden, so it is hard to generate efficient emission by direct excitation. The doping of rare earth ions into special matrices such as metallic oxides and oxysalts is traditionally an efficient method to obtain excellent luminescent material. In these kinds of phosphors, the host absorption is the main energy origin for the energy transfer and sensitization of the luminescence of active rare earth ions. Besides, the charge transfer states between rare earth ions and their

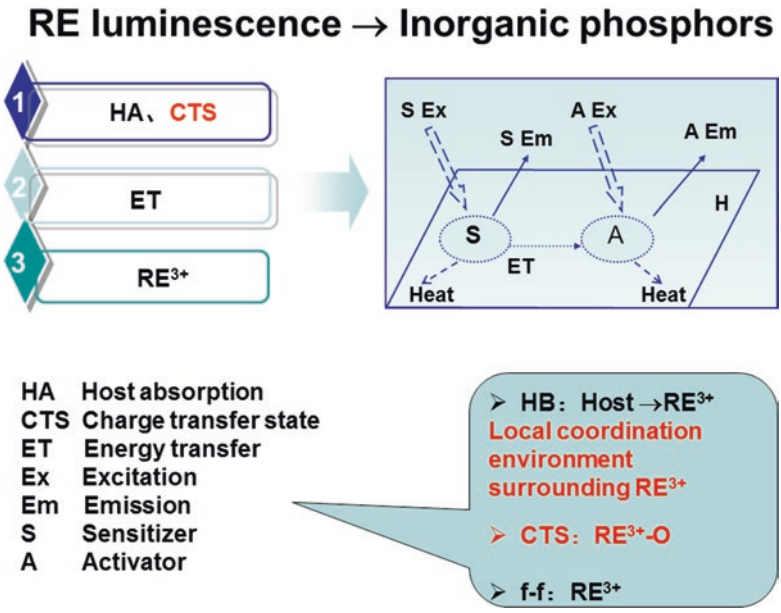

Fig. 1.3 The scheme for the luminescence and energy transfer process in rare earth solid-state phosphors

coordinated oxygen atoms (CTS) also exist in some special phosphor systems. The two main wide energy absorptions can be further excited to activate rare earth ions, resulting in the effective luminescence. Certainly, the f–f transition absorption of rare earth ions themselves also appears (Fig. 1.3).

The binary rare earth compounds used as hosts for the luminescence of rare earth ions mainly include rare earth oxides and fluorides. Among them Y_2O_3:Eu^{3+} is the most famous one because it is used as the red color phosphor for trichromatic lamp. Besides, La_2O_2S:Eu^{3+} is an important cathode ray-luminescent phosphor applied in color television. The binary rare earth fluoride can be used as the host to activate the luminescence of rare earth ions with visible or NIR emission. But their luminescent performance is not satisfied. Recently, the ternary or quaternary fluorides become the important hosts for special luminescence of rare earth ions, including $MREF_4$ (M = Na, Li), $BaREF_5$, $BaMgF_4$, K_3MF_7 (M = Zr, Hf) Na_3ScF_6, M_2NaScF_6 (M = K, Rb, Cs), and $Na_3Li_3Sc_2F_{12}$**,** While the most popular one is the $NaREF_4$ series, especially $NaYF_4$, which is a good host for the upconversion luminescence.

The most extensively used host species are the rare earth oxysalts (complex oxides), which are very abundant and versatile, including silicate, vanadate, niobate, tantalate, titanate, borate, aluminate, tungstate, molybdate, and so on. These oxysalts with oxide polyhedron frameworks can produce the effective host photoabsorption to further sensitize the luminescence of photoactive rare earth ions. In some rare earth ion (such as Eu^{3+})-doped systems, the charge transfer process can occur between Eu^{3+} ion and the oxygen center of the oxide framework, resulting in

a wide charge transfer band (CTB). This is beneficial for the energy transfer and luminescence sensitization of rare earth ions. Besides, the characteristic f–f transition of photoactive rare earth ion can also be observed. Some host systems belong to self-activated phosphors, such as tungstate. The doping of activator ions may exhibit the emissions of both host and activator; different luminescence color can be integrated to realize white light output.

Rare earth silicate phosphors include many different types, such as oxygen-rich silicon oxides RE_2SiO_5 (especially Y_2SiO_5), oxyapatites $M_2RE_8(SiO_4)_6O_2$ (M = Mg, Ca, Sr), $Ca_4RE_6(SiO_4)_6O$ (M = Ca, Sr), Zn_2SiO_4, Zr_2SiO_4, $CaSiO_3$, $Sr_3La_6(SiO_4)_6$, $Na_3RESi_3O_9$, $CaAl_2SiO_7$, etc. And also they can form $M_5RE_5(SiO_4)_3(PO_4)_3O_2$ (M = alkali earth) with other oxysalts such as PO_4^{3-}. Rare earth aluminates include $REAlO_3$: Eu^{3+}, $RE_3Al_5O_{12}$, $MREAlO_4$, MAl_2O_4, $BaMgAl_{11}O_{17}$, $Sr_4Al_{14}O_{25}$, MAl_2O_4, $MREAlO_4$, etc. Among them the most important one is yttrium aluminate garnet $Y_3Al_5O_{12}$ (YAG). Besides, the famous green and blue color phosphors are in trichromatic systems, $MAl_{11}O_{19}$:Ce^{3+}, Tb^{3+} (CAT), and $BaMg_2Al_{16}O_{27}$:Eu^{2+}(Mn^{2+}) (BAM). Rare earth borates include $REBO_3$, RE_3BO_6, $Zn_4B_6O_{13}$, MB_6O_{10} (M = alkali earth), $REAl_3(BO_3)_4$, etc. Certainly, both aluminate and borate can be introduced into the same phosphor system, such as $REAl_3(BO_3)_4$, due to their similar physical properties.

The main rare earth vanadates are $REVO_4$ and $M_3RE(VO_4)_3$, respectively. Among them YVO_4: Eu^{3+} is an important phosphor. Certainly, rare earth ions and vanadate ions can be replaced by other similar valence anions or cations, resulting in new phosphors such as $REP_xV_{1-x}O_4$ or $Bi_xRE_{1-x}VO_4$. Rare earth niobate and tantalate phosphors include many systems such as $RENbO_4$, $RETaO_4$, $Zn_3Nb_2O_8$, and $REVTa_2O_9$, respectively. Rare earth phosphates include $REPO_4$, $Zn_3(PO_4)_2$, La_3PO_7, $M_3Ln(PO_4)_3$, NH_4ZnPO_4, etc.

Rare earth tungstates belong to self-activated phosphors, which show strong blue luminescence. The rare earth-doped tungstate phosphors include $M'WO_4$: Eu/Tb (M' = Ca, Sr, Ba, Pb, Zn, Mn, Fe, Cd), RE_2WO_6, Bi_2WO_6, Ag_2WO_4, and $Ag_2W_2O_7$. The most common rare earth molybdate is $NaRE(MoO_4)_2$ (and $Na_5Lu(MoO_4)_4$). Besides, there are other systems, such as $MMoO_4$ (M = Ca, Sr, Ba, Pb, Zn, Mn, Fe, Cd) and $RE_2(MoO_4)_3$. For rare earth titanates, the main host species include $MTiO_3$ (M = Ca, Sr), $RE_2Ti_2O_7$, $RE_2Ti_2O_7$, $NaRETi_2O_6$, and $Na_2RE_2Ti_3O_{10}$, whose main activator ions are Pr^{3+} or Eu^{3+}.

1.5 Luminescent Rare Earth Coordination Compounds

Rare earth coordination compounds or complexes cover different coordination numbers from 3 to 12 and structures from zero-dimensional to three-dimensional for rare earth ions with large ion radius. A majority of them are the complexes with oxygen as the coordinated atom, whose ligands involve carboxylic acids, β-diketones, macrocyclic compounds, etc. Most of these ligands are photoactive due to their localized conjugated structure which can produce the electron transition. β-Diketones

possess the double ketone groups linked with methylene group to produce the chelation with rare earth ions. The well-known β-diketones contain acetylacetone (AcAc), trifluoroacetone (TFA), hexafluoroacetone (HFA), 2-thenoyltrifluoroacetone (TTA), dibenzoylmethane (DBM), etc. The introduction of unsymmetrical substituted groups can enhance the photoactive absorption; in particular, TTA is the best ligand to sensitize the luminescence of Eu^{3+}. The coordination interaction is simple between rare earth ions and β-diketones, mainly the chelated coordination. Generally, the β-diketone ligands transform to their enol structure (so-called keto–enol tautomerism) and lose one proton under alkali environment to form β-diketonate, which is coordinated to rare earth ions to form rare earth tris- or tetrais-β-diketonates. The macrocyclic compounds, such as crown ether, calixarene, Schiff base, etc., also can be used as ligands of rare earth ions, whose luminescent performance is not eminent but they can be used for special purposes. The most abundant ligand for rare earth ions is carboxylic acid, especially the aromatic carboxylic acid for the photofunctional application. These ligands contain one or multi-carboxylic groups or other substituted groups, which provide the abundant coordination positions for rare earth ions. Particularly, the complicated coordination modes of carboxylic groups to RE^{3+} endow their complexes with the diverse structures, always resulting in polymeric structures (1D chain, 2D layer, or 3D network). Especially the porous coordination polymers (PCPs) or metal–organic frameworks (MOFs) attract wide interest.

As we all know, all rare earth ions only possess weak light absorption because the molar absorption coefficients of most transitions in the absorption spectra of RE^{3+} are smaller than 10 $Lmol^{-1}$ cm^{-1}; only a very limited amount of radiation is absorbed by direct excitation in the 4f levels to obtain weak luminescence. To overcome this disadvantage, Weissman has discovered "*antenna effect" within the* rare earth complexes of organic ligands, which is based upon the excitation in an absorption band of the organic ligand and the subsequent intramolecular energy transfer between the organic ligands and rare earth ions [15]. Afterward, the mechanism of the energy transfer is studied in detail, putting emphasis on the rare earth β-diketonate complexes, because they are potentially active species in liquid lasers. Combining with luminescence process of organic ligands and the results in rare earth organic complexes, the commonly accepted mechanism by Crosby and Whan is shown in the inset of Fig. 1.4 [16, 17]. Upon irradiation with ultraviolet radiation, organic molecules are excited to a vibrational level of the excited singlet state (S_i) and then may undergo fast internal conversion process (IC) to relax to the lowest vibrational level of the S_1 state, which is a very quick process and easily occurs in solution for the interaction with solvent molecules. Commonly, the excited singlet state of organic molecule can be deactivated radiatively to the ground state, resulting in molecular fluorescence with the spin which allows transition between two electronic states with the same spin multiplicity from S_1 to S_0. On the other hand, the excited singlet state may occur as conversion with different spin multiplicity from singlet S_i to triplet T_i by the microscopic quantum mechanics perturbation, called intersystem crossing (ISC). The excited triplet state of organic molecule can be deactivated radiatively to the singlet ground state, resulting in molecular

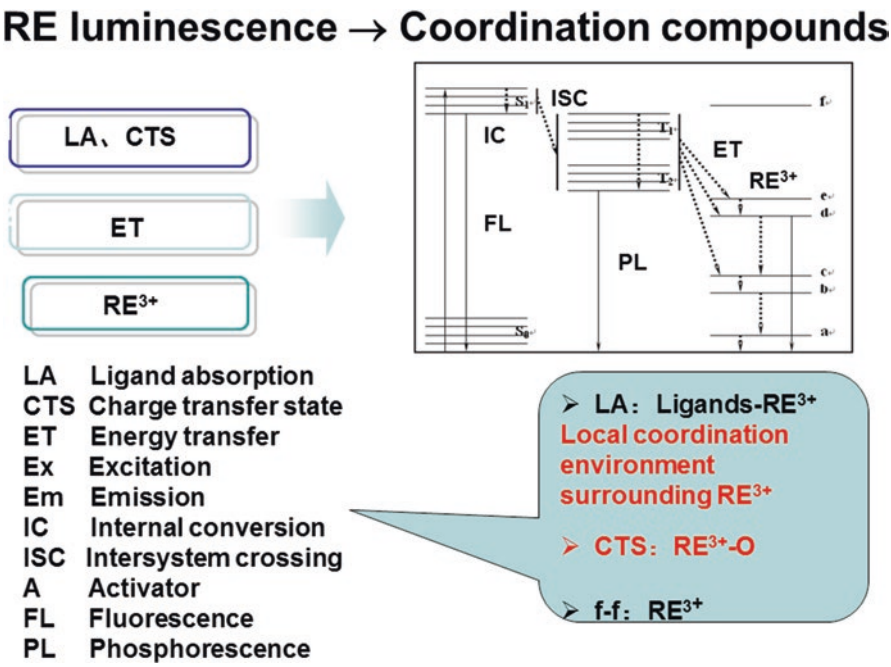

Fig. 1.4 The scheme for the luminescence and energy transfer process in rare earth coordination compounds

phosphorescence with the spin-forbidden transition from T_1 to S_0. When organic molecule behaves like a ligand in rare earth complexes through coordination interaction, the complex may undergo a non-radiative transition from the triplet state to an excited state of the rare earth ion through a so-called intramolecular energy transfer process. The sensitized rare earth ion may undergo a radiative transition to a lower 4f state by characteristic line-like photoluminescence or may be deactivated by non-radiative processes to produce heat. From the emission transition position of common rare earth ions, the certain resonance emission levels can be determined, which are $^4G_{5/2}$ for Sm^{3+} (17,800 cm^{-1}), $^5D_0$ for Eu^{3+} (17,250 cm^{-1}), $^5D_4$ for Tb^{3+} (20,500 cm^{-1}), and $^4F_{9/2}$ for Dy^{3+} (20,960 cm^{-1}), respectively. If the rare earth ion is excited to a non-emitting level, the excitation energy is dissipated via non-radiative processes until a resonance level is reached either directly by excitation in the 4f levels or indirectly by energy transfer. In this case, radiative transitions will compete with the non-radiative processes to display RE^{3+}-centered emission. So the final line emission of rare earth ion depends on the minimization of non-radiative deactivation or other emissions of molecular fluorescence and phosphorescence. To populate a resonance level of a RE^{3+} ion, the necessary prerequisite is the lowest triplet state of the ligand, or the complex is higher than the resonant energy level of the rare earth ion. If not, no effective emission of RE^{3+} is found, and molecular luminescence (fluorescence or phosphorescence) may be observed. So the intramolecular

energy transfer within the rare earth complexes may depend on the match between the energy of the lowest triplet level of the ligands or complexes and the resonance level of RE^{3+}. Because the position of the triplet level depends on the type of ligand, it is therefore possible to control the luminescence intensity observed for a given rare earth ion by variation of the ligand.

Sato and Wada have investigated the relationship between the intramolecular energy transfer efficiencies and triplet state energies in the rare earth β-diketones chelates [18]. Gadolinium complexes are selected as model complexes for the determination of the lowest triplet state energies of organic ligands due to their enhanced phosphorescence/fluorescence ratios ($\Phi_{ph}/\Phi_{fl} > 100$) compared to those of other rare earth complexes, and the emitting level energy of Gd^{3+} is so much higher than the triplet state energies of organic ligands; therefore, it cannot be sensitized by ligands. Moreover, the presence of a heavy paramagnetic Gd^{3+} ion enhances the ISC from the singlet to the triplet state because of the mixing of the triplet and singlet states, so-called *paramagnetic effect*. The spin–orbit coupling interaction endows the triplet state a partially singlet character to relax the spectral selection rules. The efficiency of the energy transfer is proportional to the overlap between the phosphorescence spectrum of the ligand and the absorption spectrum of the rare earth ion. The overlap decreases as the triplet state energy increases. Therefore, the intramolecular energy migration efficiency from the organic ligands to the central RE^{3+} is the most important factor influencing the luminescence properties of rare earth complexes, which depends mainly on the two energy transfer processes. One is from the lowest triplet state energy of organic ligand to the resonant energy level by Dexter's resonant exchange interaction theory (Eq. 1.1) [19]:

$$k_{ET} = 2\pi Z^2 \int F_d(E) F_a(E) \mathrm{dE} \exp\left(-2R_{da}/L\right) \tag{1.1}$$

Where k_{ET} is the rate constant of the intermolecular energy transfer and P_{da} is the transition probability of the resonant exchange interaction. $2\pi Z^2/R$ is the constant relating to the specific mutual distance between the central RE^{3+} ion and its coordinated atoms. $F_d(E)$ and $E_a(E)$ are the experimental luminescent spectrum of energy donor (ligands) and the experimental absorption spectrum of energy acceptor (RE^{3+}), respectively, R_{da} is the intermolecular distance between donor atoms and acceptor atoms, and L is the van der Waals radius. Both R_{da} and L may be considered to be constant in intramolecular transfer processes, so k_{ET} is proportional to the overlap of $F_d(E)$ and $E_a(E)$.

On the other hand, a close match between the energy of the triplet state and the energy of the receiving 4f level of the rare earth ion is not desirable either, because energy back transfer of the rare earth ion to the triplet state can occur. When the energy transfer is not very efficient, it is possible to observe some remaining ligand emission in combination with the rare earth-centered emission. The inverse energy transition by the thermal deactivation mechanism is shown as follows (Eq. 1.2) [20, 21]:

$$k(T) = A\exp(-\Delta E / RT) \tag{1.2}$$

Both of them represent the overlap spectrum of RE^{3+}. With the decrease in the energy difference between the triplet state energy of conjugated carboxylic acid and RE^{3+}, the overlap of $F_d(E)$ and $E_a(E)$ is increased. So from the above equation, it can be concluded that the larger the overlap between the luminescent spectrum of organic ligands and the emissive energy of RE^{3+}, the larger is the intramolecular energy rate constant k_{ET}. On the other hand, the activation energy ΔE in Eq. (1.2) is equal to the energy difference $\Delta E(\text{Tr-RE}^{3+})$, while from the formula, the inverse energy transfer rate constant $k(T)$ increased with decreasing $\Delta E(\text{Tr-RE}^{3+})$ [22–25]. As discussed above, there should exist an optimal energy difference between the triplet position of organic ligands and the emissive energy level RE^{3+}; a larger or a smaller $\Delta E(\text{Tr-RE}^{3+})$ will decrease the luminescence of rare earth complexes.

Another possibility to sensitize rare earth luminescence is via *charge transfer states* [26–28]. This is especially the case for trivalent rare earth ions that can easily be reduced to the divalent state (redox-sensitive rare earth ions) like Sm^{3+}, Eu^{3+}, and Yb^{3+}, where light can be absorbed by an intense ligand-to-metal charge transfer state (LMCT state) from which the excitation energy can be transferred to the 4f levels of the rare earth ion. This process only works well if the LMCT state lies at high-enough energy. For instance, sensitization of Eu^{3+} through a LMCT state is efficient if the LMCT lies above 40,000 cm^{-1}. Low-lying LMCT states will partially or totally quench the luminescence. In the case of Eu^{3+}, metal-centered luminescence is totally quenched if the LMCT energy is less than 25,000 cm^{-1} [29]. Also strongly absorbing chromophores containing d-block metals can be used for sensitizing rare earth luminescence [30]. Because these chromophores absorb in general at longer wavelengths than the most often used organic chromophores (typically in the visible spectral region), *d-block chromophores* are especially useful for sensitizing the near-infrared luminescence of rare earth ions like Nd^{3+}, Er^{3+}, and Yb^{3+}.

Besides, Kleinerman proposes a mechanism of direct transfer of energy from the excited singlet state S_1 to the energy levels of the rare earth ion [31], which is now not considered to be of great importance because it is often not efficient due to the short lifetime of the excited singlet state. In this way, the energetic constraints from the T_1 state of the ligand can be avoided. Horrocks and co-workers later examine the energy transfer processes in rare earth ion-binding proteins and assume that it is the excited singlet state of the chromophore that sensitizes the rare earth examine [6]. However, owing to the lack of information regarding the emission from the excited states of the coordinated ligand and the difficulties in the determination of the ligand-localized triplet–triplet absorption spectra for rare earth chelates, it has been very difficult to prove for certain which state is responsible for the energy transfer process [32]. All the experimental work conducted on the sensitization of rare earth chelate luminescence seems to support the triplet pathway, whereas the singlet pathway for the sensitization of the Eu complex has not been observed experimentally [32]. Yang et al. report the successful extension of the excitation window to the visible region for a Eu complex, which subsequently exhibits highly

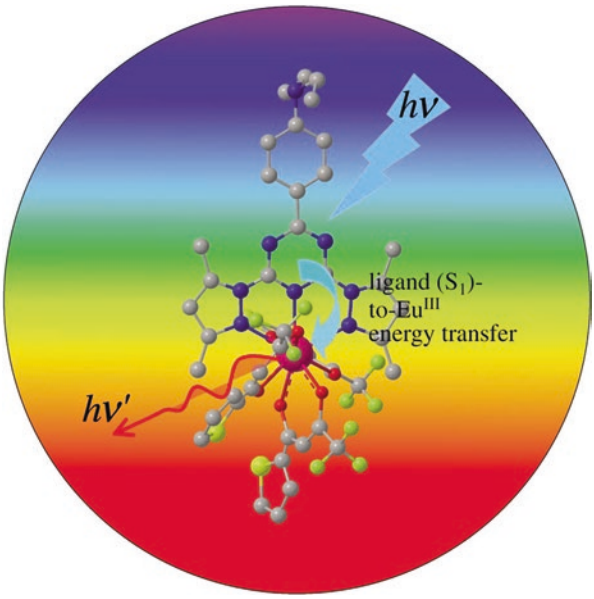

Fig. 1.5 The scheme for the singlet direct energy transfer pathway diagram (bottom) in complex Eu(TTA)3 L (L = N,N-dialkyl aniline moiety-modified dipyrazolyltriazine derivative) (Reprinted with permission from Ref. [32]. Copyright 2004 John Wiley & Sons Ltd)

efficient EuIII-centered luminescence. The sensitization mechanism is shown to take place through the singlet pathway by means of time-resolved luminescence spectroscopic studies. They have demonstrated the first observable case of excitation energy transfer from the ligand to the luminescent states of EuIII ion through the singlet pathway in a visible light-sensitized europium complex. The excitation window for this complex has been extended up to 460 nm (Fig. 1.5).

In addition, in ternary rare earth complexes, there also exists the energy transfer between different ligands. According to the phosphorescent spectra or lifetimes of ternary and binary gadolinium complexes, it can be found that in some ternary rare earth complexes, only one ligand may become the main energy donor for the energy transfer from another ligand to this ligand, whose energy transfer also depends on the triplet state energy level of the two ligands. This phenomenon often occurs in the ternary rare earth complexes with aromatic carboxylic acids and heterocyclic ligands [33]. On the other hand, some inert RE ions (La^{3+}, Gd^{3+}, Y^{3+}, Lu^{3+}) also enhance ultraviolet absorption intensity of ligands and then enhance phosphorescence intensity to improve intersystem crossing efficiency from S_1 to T_1 of ligands. Subsequently, the intramolecular energy transfer efficiency from ligands to RE^{3+} will be increased to obtain the strong luminescence of RE^{3+} [34].

1.6 Photofunctional Rare Earth Hybrid Materials

Photofunctional rare earth hybrid materials are more complicated than molecular systems. The initial aim is to prepare the multicomponent materials and modify their properties, such as thermal stability or photostability. But now the photofunctional hybrid materials are endowed with the abundant connotations. These hybrids display special characteristics of both solid-state luminescence and molecular luminescence. The hybrids not only involve the structural components as the building units but also contain the photofunctional units. The aggregate state and microstructure of the photofunctional hybrid materials have been studied, and the final aim is to realize the property tuning and function integration. In these photofunctional rare earth hybrid systems, all kinds of interaction forces are involved, including coordination bonds, covalent bonds, and other interactions. On the other hand, the composition of hybrid materials is multi-scale, from molecular scale to nanoscale and to bulk materials.

As the above discussion attests, the luminescent rare earth compounds mainly have two types: one is the atomic or ionic system, i.e., rare earth solid-state compounds as phosphors (continuous solids), and the other is the molecular system, i.e., rare earth coordination compounds or complexes (molecular solids). The main distinction between the luminescence of the two kinds of compounds is different energy donors, i.e., host absorption for the former and ligand absorption for the latter. But in fact, the nature of the interaction between photoactive rare earth ions and hosts or ligands is identical, which is the coordination and depends on the coordination environment surrounding rare earth ions. Certainly, the charge transfer state absorption also exists between certain rare earth ions and ligand or host, such as Eu^{3+}-O CTS.

For rare earth photofunctional hybrid materials, the initial aim is only to put photoactive species (mainly rare earth complexes) into some hosts to improve their thermal or photostability [35–39]. The combination of organic and inorganic components at a molecular or nanometer scale integrates certain strong points of organic compounds (easy processing with conventional techniques, elasticity, and organic functionalities) with the advantages of inorganic components (hardness, thermal and chemical stabilities). According to the different interaction forces between the two phases, these hybrid materials are divided into two major classes [40]. Physically doped hybrids have weak interactions (such as hydrogen bonding, van der Waals forces, or weak static effects) between the organic and inorganic phases, which cannot overcome many problems such as clustering of emitters, inhomogeneous dispersion of the components, or leaching of the dopants [41–46]. Chemically bonded hybrids have strong interactions such as covalent, ion–covalent, coordination, or Lewis acid/base bonds, which can graft the rare earth complexes onto hosts [47, 48]. The latter class of hybrids overcome the disadvantages of the former one, since they are homogeneous and can avoid the self-quenching of rare earth ions, which results in increased incorporation concentrations.

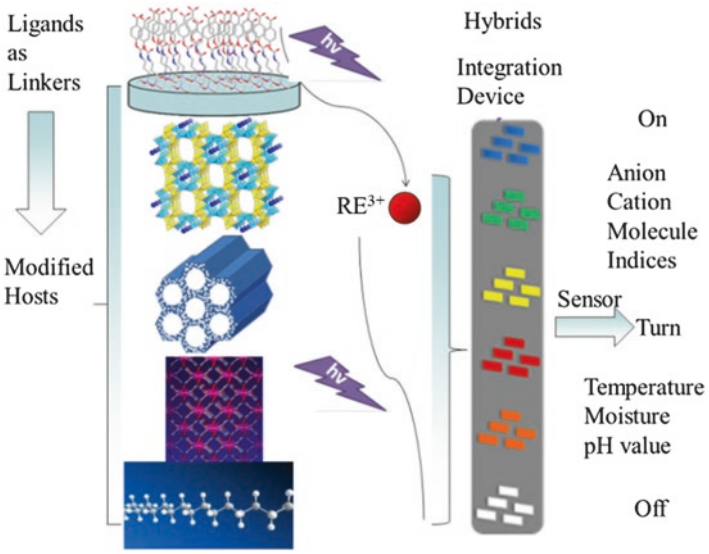

Fig. 1.6 The scheme for the compositions and photophysical applications of photofunctional rare earth hybrid materials

Further, it needs to mention the nature of the luminescence and its significance for photofunctional hybrid materials. The whole photofunctional hybrid material system belongs to the complicated frameworks or networks that contain various kinds of building blocks. The important component is the ligand or linker functionalized host. The scheme of the photofunctional hybrid systems is shown in Fig. 1.6. The linker is a special ligand which plays a key role in producing the antenna effect to transfer energy to sensitize the luminescence of coordinated photoactive RE^{3+}. The linker functionalized host in the hybrid system shows the characteristics of both of the ligand and the host, which integrates the luminescence of solid-state phosphors and molecular complexes. The common hosts include sol–gel-derived silica, which is mainly from organically modified silane, mesoporous silica, microporous zeolite, metal–organic framework or porous coordination polymer, organic polymer or its composites, etc. Certainly, the photo-absorption is often affected by the metal ions coordinated to linker-modified hosts in some systems such as MOFs (or PCPs). The final hybrid system can display multicolor luminescence under energy transfer with antenna effect and also achieve the white color luminescence integration. Some hybrids can be further studied to explore their application in sensing.

In this book, seven topics are discussed in the following chapters. Chapter 2 focuses on photofunctional rare earth hybrid materials based on sol–gel-derived silica, mainly with the organically modified silanes as the linkers. Chapter 3 focuses on photofunctional rare earth hybrid materials based on organically modified mesoporous silica. Chapter 4 focuses on photofunctional rare earth hybrid materials based on microporous zeolite. Chapter 5 focuses on photofunctional rare earth hybrid materi-

als based on metal–organic frameworks. Chapter 6 focuses on photofunctional rare earth hybrid materials based on organic polymer or its composites. Chapter 7 focuses on photofunctional rare earth hybrid materials with other functional units achieved by multicomponent assembly. Chapter 8 focuses on the photophysical applications of photofunctional rare earth hybrid materials, especially on chemical sensing. The seven topics are chosen because there are extensive reports on them.

References

1. Ropp RC (2004) Luminescence and the solid state, 2nd edn. Elsevier Science, Boston
2. Jolly L (1984) Modern inorganic chemistry. McGraw-Hill, New York
3. Kitai A (2008) Luminescent materials and applications. Wiley, Hoboken
4. Yan B, Chen ZD (2001) Cyano-bridged aqua (N,N-dimethylacetamide) (cyanoiron) rare earths from samarium, gadolinium or holmium nitrate and potassium hexacyanoferrate: crystal structure and magnetochemistry. Helv Chim Acta 84:817–829
5. Yan B, Wang SX, Chen ZD (2003) Synthesis, crystal structures and magnetic properties of ion-pair complexes with hydrogen bonding network: $ln(DMA)_n(H_2O)_mCr(CN)_6{\cdot}xH_2O$ (for ln = Sm, Gd: n = 4, m = 3, x = 2; for ln = Er: n = 3, m = 4, x = 0). J Coord Chem 55:573–586
6. JH W, Yan B (2010) Room-temperature solid-state reaction behavior, hydrothermal crystallization and physical characterization of $NaRE(MoO_4)_2$ and $Na_5Lu(MoO_4)_4$ compounds. J Amer Ceram Soc 93:2188–2194
7. Moore EG, Samuel APS, Raymond KN (2009) From antenna to assay: lessons learned in lanthanide luminescence. Acc Chem Res 42:542–552
8. Blasse G, Grabmaier BC (1994) Luminescent materials. Springer, Berlin
9. Blasse G (1992) Vibronic transitions in rare earth spectroscopy. Int Rev Phys Chem 11:71–100
10. Carnall WT, Fields PR, Rajnak K (1968) Electronic energy levels of the trivalent lanthanide aquo ions. IV. Eu^{3+}. J Chem Phys 49:4450–4455
11. Carnall WT, Fields PR, Rajnak K (1968) Electronic energy levels of the trivalent lanthanide aquo ions. III. Tb^{3+}. J Chem Phys 49:4447–4449
12. Carnall WT, Fields PR, Rajnak K (1968) Electronic energy levels in the trivalent lanthanide aquo ions. I. Pr^{3+}, Nd^{3+}, Pm^{3+}, Sm^{3+}, Dy^{3+}, Ho^{3+}, Er^{3+}, and Tm^{3+}. J Chem Phys 49:4424–4442
13. Di Bartolo B (1968) Optical interactionin solids. Wiley, New York
14. Blasse G, Dirksen GJ, Meijerink A (1990) The luminescence of ytterbium(II) in strontium tetraborate. Chem Phys Lett 167:41–44
15. Weissman SI (1942) Intramolecular energy transfer: the fluorescence of complexes of europium. J Chem Phys 10:214–217
16. Crosby GA, Whan RE, Alire RM (1961) Intramolecular energy transfer in rare earth chelates–role of the triplet state. J Chem Phys 34:743–748
17. Crosby GA, Whan RE, Freeman J (1962) Spectroscopic studies of rare earth chelates. J Phys Chem 66:2493–2499
18. Sato S, Wada M (1970) Relations between intramolecular energy transfer efficiencies and triplet state energies in rare earth β-diketone chelates. Bull Chem Soc Jpn 43:1955–1962
19. Dexter DL (1953) A theory of sensitized luminescence in solids. J Chem Phys 21:836–850
20. Brown TD, Shepherd TM (1973) Factors affecting the quantum efficiencies of fluorescent terbium(III) chelates in the solid state. J Chem Soc Dalton Trans:336–341
21. Balzani V, Moggi L, Manfrin MF, Bolletta F (1975) Quenching and sensitization process of coordination compounds. Coord Chem Rev 15:321–433
22. SL W, YL W, Yang YS (1992) Rare earth(iii) complexes with indole-derived acetylacetones II. Luminescent intensity for europium(iii) and terbium(iii) complexes. J Alloys Compd 180:399–402

23. Song YS, Yan B, Chen ZX (2004) Different crystal structure and photophysical properties of rare earth complexes with 5-bromonicotinic acid. J Solid State Chem 177:3805–3814
24. Yan B, Zhou B Photophysical properties of dysprosium complexes with aromatic carboxylic acids by molecular spectroscopy. J Photochem Photobiol A Chem 171:181–186
25. Wang QM, Yan B, Zhang XH (2005) Photophysical properties of novel rare earth complexes with long chain mono-eicosyl *cis*-butene dicarboxylate. J Photochem Photobiol A Chem 174:119–124
26. Petoud S, Bunzli JCG, Glanzman T, Piguet C, Xiang Q, Thummel RP (1999) Influence of charge-transfer states on the Eu(III) luminescence in mononuclear triple helical complexes with tridentate aromatic ligands. J Lumin 82:69–79
27. Faustino WM, Malta OL, de Sa GF (2005) Intramolecular energy transfer through charge transfer state in lanthanide compounds: a theoretical approach. J Chem Phys122:317–325
28. Daleo A, Picot A, Beeby A, Williams JAG, Le Guennic B, Andraud C, Maury O (2008) Efficient sensitization of europium, ytterbium, and neodymium functionalized tris-dipicolinate lanthanide complexes through tunable charge-transfer excited states. Inorg Chem 47:10258–10268
29. Fonger WH, Struck CW (1970) Eu^{3+} ^5D resonance quenching to the charge-transfer states in Y_2O_2S, La_2O_2S, and LaOCl. J Chem Phys 52:6364–6371
30. Ward MD (2007) Transition-metal sensitized near-infrared luminescence from lanthanides in d-f heteronuclear arrays. Coord Chem Rev 251:1663–1677
31. Kleinerman M (1964) Energy migration in lanthanide chelates. Bull Am Phys Soc *9*:265–269
32. Yang C, LM F, Wang Y, Zhang JP, Wong WT, Ai XC, Qiao YF, Zou BS, Gui LL (2004) A highly luminescent europium complex showing visible-light-sensitized red emission: direct observation of the singlet pathway. Angew Chem Int Ed 43:5010–5013
33. Yan B, Zhang HJ, Wang SB, Ni JZ (1998) Intramolecular energy transfer mechanism between ligands in ternary complexes with aromatic acids and 1,10-phenanthroline. J Photochem Photobiol A Chem 116:209–214
34. Yang JH, Zhu GY, Wang H (1989) Application of the co-luminescence effect of rare earths: simultaneous determination of trace amounts of samarium and europium in solution. Analyst 114:1417–1419
35. Carlos LD, Ferreira RAS, Bermudez VD, Ribeiro JLS (2009) Rare earth-containing light-emitting organic–inorganic hybrids: a bet on the future. Adv Mater 21:509534
36. Binnemans K (2009) Rare earth-based luminescent hybrid materials. Chem Rev 109:42834374
37. Yan B (2012) Recent progress on photofunctional rare earth hybrid materials. RSC Adv 2:9304–9324
38. Feng J, Zhang HJ (2013) Hybrid materials based on rare earth organic complexes: a review. Chem Soc Rev 42:387–410
39. Zhang HJ, Niu CJ, Feng J (2014) Rare earth organic-inorganic hybrid luminescent materials. Scientific Press. (in Chinese)
40. Sanchez C, Ribot F (1994) Design of hybrid organic-inorganic materials synthesized via sol-gel chemistry. New J Chem 18:1007–1047
41. Yan B, Zhang HJ, Wang SB, Ni JZ (1997) Luminescence properties of the ternary rare earth complexes with *beta*-diketones and 1,10-phenanthroline incorporated in silica matrix by a sol-gel method. Mater Chem Phys 51:92–96
42. Tanner PA, Yan B, Zhang HJ (2000) Preparation and luminescence properties of sol-gel hybrid materials incorporated with europium complexes. J Mater Chem 35:4325–4328
43. Yan B, Wang QM (2004) In-situ composition and luminescence of terbium coordination polymers/PEMA hybrid thick films. Opt Mater 27:533–537
44. LS F, Meng QG, Zhang HJ, Wang SB, Yang KY, Ni JZ (2000) In situ synthesis of terbium-benzoic acid complex in sol-gel derived silica by a two-step sol-gel method. J Phys Chem Sol 61:1877–1881
45. Dang S, Sun LN, Zhang HJ, Guo XM, Li ZF, Feng J, Guo HD, Guo ZY (2008) Near-infrared luminescence from sol-gel materials doped with holmium(III) and thulium(III) complexes. J Phys Chem C 112:13240–13247

46. Pecoraro E, Ferreira RAS, Molina C, Ribeiro SJL, Messsaddeq Y, Carlos LD (2008) Photoluminescence of bulks and thin films of Eu^{3+}-doped organic/inorganic hybrids. J Alloys Compds 451:136–139
47. Franville AC, Zambon D, Mahiou R (2000) Luminescence behavior of sol−gel-derived hybrid materials resulting from covalent grafting of a chromophore unit to different organically modified alkoxysilanes. Chem Mater 12:428–435
48. Minoofar PN, Hernandez R, Chia S, Dunn B, Zink JI, Franville AC (2002) Placement and characterization of pairs of luminescent molecules in spatially separated regions of nanostructured thin films. J Am Chem Soc 124:14388–14396